ACKNOWLEDGMENT

The authors thank Dr. J. H. Wang for his helpful discussions and constant encouragement.

REFERENCES

1. J. Schutt-Aine, Static analysis of V-transmission lines, IEEE Trans Microwave Theory Techn MTT-40 (1992), 659–663.
2. N. Yuan, C. Ruan, and W. Lin, Analytical analyzes of V, elliptic, and circular-shaped microshield transmission lines, IEEE Trans Microwave Theory Techn MTT-42 (1994), 855–859.
3. O.M. Ramahi, A.Z. Elsherbeni, and C.E. Smith, Dynamic analysis of V transmission lines, IEEE Trans Components Packaging Techn Part B 21 (1998), 250–257.
4. K.J. Herrick, T.A. Schwarz, and L.P.B. Katehi, Si-micromachined coplanar waveguides for use in high-frequency circuits, IEEE Trans Microwave Theory Techn MTT-46 (1998), 762–768.
5. R.N. Simons, Coplanar waveguide circuits, components and systems, Wiley, New York, 2001.
6. X. Zhang and K.K. Mei, Time-domain finite-difference approach for the calculation of the frequency-dependent characteristics of microstrip discontinuities, IEEE Trans Microwave Theory Techn MTT-36 (1988), 1775–1787.
7. X. Zhang, J. Fang, K.K. Mei, and Y. Liu, Calculation of the dispersive characteristics of microstrips by the time-domain finite difference method, IEEE Trans Microwave Theory Techn MTT-36 (1988), 263–26.
8. G.-C. Liang, Y.-W. Liu, and K.K. Mei, Full-wave analysis of coplanar waveguide and slotline using the time-domain finite-difference method, IEEE Trans Microwave Theory Techn MTT-37 (1989), 1949–1957.
9. D.M. Sheen, S.M. Ali, M.D. Abouzahra, and J.A. Kong, Application of the three-dimensional finite-difference time-domain method to the analysis of planar microstrip circuits, IEEE Trans Microwave Theory Techn MTT-38 (1990), 849–856.
10. M.J. Piket-May, A. Taflove, and J. Baron, FDTD modeling of digital signal propagation in 3-D circuits with passive and active loads, IEEE Trans Microwave Theory Techn MTT-42 (1994), 1514–1523.
11. A. Tafove and S.C. Hagness, Computational electromagnetics: The finite-difference time-domain method, 2nd ed., Artech House, Boston, 2000.
12. P. Mezzanotte, L. Poselli, and R. Sorrentino, A simple way to model curved metal boundaries in FDTD algorithm avoiding staircase approximation, IEEE Microwave Guide Wave Lett 5 (1995), 267–269.
13. M. Lahti, V. Lantto, and S. Leppavuori, Planar inductors on an LTCC substrate realized by the gravure-offset-printing technique, IEEE Trans Compon Techn 23 (2000), 606–610.
14. H. Jantunen, R. Rautioaho, A. Uusimaki, and S. Leppavuori, Compositions of $MgTiO_3$-$CaTiO_3$ ceramic with two borosilicate glasses for LTCC technology, J Euro Ceram Soc 20 (2000), 2331–2336.
15. D. Heo, A. Sutono, E. Chen, Y. Suh, and J. Laskar, A 1.9-GHz DECT CMOS power amplifier with fully integrated multilayer LTCC passives, IEEE Micro Wireless Compon Lett 11 (2001), 249–251.
16. K. Kageyama, K. Saito, H. Murase, H. Utaki, and T. Yamanoto, Tunable active filters having multilayer structure using LTCC, IEEE Trans Microwave Theory Techn MTT-49 (2001), 2421–2424.

AN EXTENSION OF THE ARRAY DECOMPOSITION METHOD FOR LARGE FINITE-ARRAY ANALYSIS

Rick Kindt, K. Sertel, E. Topsakal, and J. L. Volakis
Radiation Lab
University of Michigan
Ann Arbor, MI 48109-2122

Received 10 February 2003

ABSTRACT: *In this paper, a method is presented for analyzing very large finite arrays of tapered-slot antenna elements. The Toeplitz matrix property of regularly spaced arrays, combined with a parametrically truncated coupling radius, generates fixed matrix storage based on the coupling radius rather than array size, thus allowing very large problem analysis.* © 2003 Wiley Periodicals, Inc. Microwave Opt Technol Lett 38: 323–328, 2003; Published online in Wiley InterScience (www.interscience.wiley.com). DOI 10.1002/mop.11050

Key words: *finite array; domain decomposition; array decomposition method; finite element-boundary integral method*

1. INTRODUCTION

Large finite arrays are playing an increasingly important role in government as well as industrial applications. Of particular interest is the consideration of edge diffraction for sidelobe evaluation and scanning capabilities. However, due to the excessive storage requirements of the system matrix for large finite arrays, such analyses have been impractical for numerical analysis. At present, numerical analysis is limited to arrays of small size, depending on the antenna element complexity. As an example, consider a 150 × 150 array of antennas with individual array elements requiring 1448 unknowns (660 FEM, 788 BI) to model (32 million unknowns total). Using conventional numerical modeling tools (without the benefit of matrix reduction) the required storage is on the order of 10^{12} bytes, making it an impractical problem even for robust $O(N \log N)$ solvers. Problems of this magnitude make it necessary to develop a means of eliminating matrix storage requirements.

Much attention has already been given to techniques that lead to significant reduction in memory requirements. Among these, the conjugate gradient-fast Fourier transform (CG-FFT) method [1–4] has allowed large-scale scattering solutions of planar geometries. This technique generates a Toeplitz matrix system with storage requirements of $O(N)$ as compared to $O(N^2)$ for conventional storage. Other more general compression techniques include the adaptive integral method (AIM) [5, 6] and the multilevel fast multipole method (MLFMM) [7, 8], neither of which require evenly spaced grids or even planar geometries to achieve $O(N \log N)$ storage requirements. Nevertheless, exploitation of the Toeplitz properties in finite array problems has been shown to lead to lower memory and solution time requirements than generalized compression techniques alone [9].

Recently, a method was introduced for analyzing arrays of arbitrary elements [10]. This technique, referred to as the array decomposition method (ADM), is appropriate for array elements of arbitrary size, shape, and material, when implemented with the finite-element boundary-integral (FE-BI) method [8, 11]. Using ADM, it was demonstrated that a 30 × 30 array of small 1100-unknown TSA elements can be modeled with a

modest 16 GB of storage (versus 3.8 terabytes with conventional methods). However, like most other methods, as the array size increases, ADM is limited by matrix storage requirements [$O(nm^2)$, where n = array elements, m = element unknowns, and $N = mn$.].

In this paper, we introduce a method for the analysis of large finite arrays with benefits similar to ADM, but without the matrix storage bottleneck. Like ADM, it implements the same Toeplitz storage scheme for reducing matrix storage and fill time. However, in contrast to ADM, the method presented in this paper implements a truncated coupling radius (TCR) that removes the bottleneck of matrix storage while still maintaining a controlled degree of accuracy. This makes the accurate analysis of large finite arrays possible, even with the limited resources of desktop computers.

In this paper, we demonstrate what is necessary to characterize the coupling properties of the chosen array element in a finite-array environment. We then accurately model a small finite array using significantly reduced matrix storage, and later use the characterization of the array element's coupling properties to model a much larger finite array (150 × 150 array with 32 million unknowns), within a matter of hours.

2. GENERAL APPROACH

We begin with the reasonable assumption that coupling at any location in the finite array will be largely dominated by elements within a given radius. That is, it is reasonable to assume that two elements next to each other will have stronger coupling than two elements on opposite sides of the array. Our premise is to therefore ignore the contribution of elements located outside a pre-specified radius of influence, in order to keep the stronger contributions from nearby elements. In doing so, it is understood that some degree of approximation has been introduced. However, it is generally accepted that for large problems it becomes necessary to implement iterative solution approaches [12] that generate approximate solutions as well, and are controlled to within a certain percent error (typically 1% or so) from the exact solution. In a similar manner here, the radius of influence is chosen such that the achieved solution is within a controlled margin of error from the exact solution (such as 1–4%). Knowledge of solution accuracy versus coupling radius is predetermined through characterization of the chosen array element's coupling properties in a finite-array environment.

While the concept of throwing away weak coupling terms to reduce storage is simple in itself, when applied to an array problem in which a Toeplitz storage scheme has been implemented, extreme matrix storage savings can be achieved for larger problems. Once it has been determined that a given finite coupling radius will achieve the desired solution accuracy, the Toeplitz matrix storage requirements will depend only on the extent of this radius and not on the array size itself. As a consequence, matrix storage is no longer the limiting factor in the size of the problem we can address. Specifically, a 10 × 10 array of the chosen element may have the same matrix storage requirements as a 150 × 150 array (assuming the coupling radius does not encompass the entire 10 × 10 array). The method can be used to model more arbitrary array geometries, such as circular or elliptical arrays, as well as to treat situations with missing elements.

3. FORMULATION

We begin by considering the solution of a linear system of equations representing an antenna (or scattering) problem. The system of equations will take the form

$$[A]\{x\} = \{b\}, \tag{1}$$

where $\{b\}$ is the system excitation, $\{x\}$ represents the current coefficients, and $[A]$ is the matrix of coefficients for coupling relations within the antenna. The system of Eq. (1) can be generated using any numerical integral equation method, such as the method of moments (MoM), or preferably the finite-element boundary-integral (FE-BI) method. In our solutions, we employ an underlying FE-BI formulation to model the individual elements of the array, similar to the formulation found in [8, 10, 11]. The open domain approach of FE-BI allows us to model any type of antenna element, without restrictions to geometry or materials, while benefiting from the sparse storage of FEM.

For different problem types, the system of equations may be assembled in various ways. For an array system, we choose to expand our system of equations based on element interactions, verses the typical operator-type grouping of [8, 11]. For an M element linear array, the system of equations is expanded as

$$\begin{bmatrix} [a]_{11'} & [a]_{12'} & \cdots & [a]_{1M'} \\ [a]_{21'} & [a]_{22'} & \cdots & [a]_{2M'} \\ \vdots & \vdots & \ddots & \vdots \\ [a]_{M1'} & [a]_{M2'} & \cdots & [a]_{MM'} \end{bmatrix} \begin{Bmatrix} \{x\}_1 \\ \{x\}_2 \\ \vdots \\ \{x\}_M \end{Bmatrix} = \begin{Bmatrix} \{b\}_1 \\ \{b\}_2 \\ \vdots \\ \{b\}_M \end{Bmatrix} \Rightarrow [A]\{x\} = \{b\}, \tag{2}$$

where the sub-matrices $[a]_{mn'}$ represent the coupling sub-matrices between the volumetric antenna elements m and n' of the array, where $m, n' = 1 \cdots M$, n' is the source element. The diagonal terms of the matrix, for example, $[a]_{11'}$, are the complete FE-BI sub-matrix systems of the isolated antenna elements. Thus, $[a]_{11'}\{x\}_1 = \{b\}_1$ would be the complete FE-BI system necessary to model an isolated antenna element $n = 1$. The fields of element $n = 1$ ($\{x\}_1$) are coupled to the fields of element $n = 2$ ($\{x\}_2$) via the coupling coefficients $[a]_{21'}$. We also note that the coupling is modeled via the free-space Green's function, and thus the sub-matrix $[a]_{21'}$ consists of only boundary integral operators characterizing the interactions of surface fields on the antenna element boundaries.

Of importance in solving Eq. (2) is that, for equally spaced antenna elements with sequential numbering, the matrix system will have a Toeplitz property, due to the spatial dependence of the free-space Green's function. Therefore, the coupling sub-matrices have the property $[a]_{mm'} = [a]_{(m-m')} = [a]_p$, for any m, m' element pair, and thus only a subset of matrix terms need be stored to account for all the unique information contained in $[A]$. For instance, the system of equations for a linear array of M elements as given in Eq. (2) can be compactly stored as the following block-vector:

$$\Pi^{1D} = \{[a]_{M-1} \quad \cdots \quad [a]_1 \quad [a]_0 \quad [a]_{-1} \quad \cdots \quad [a]_{1-M}\}, \tag{3}$$

where $[a]_{mn} = [a]_{m-n} = [a]_p$ (as noted above), so that $[a]_0$ refers to the array element self matrix. This sub-matrix is comparatively small and can thus be inverted and used as a block-diagonal matrix preconditioner on the overall system $[A]$. This preconditioner was previously used in [10], and was demonstrated to achieve significant convergence improvements.

We note that for a 2D array of $M \times N$ elements, the unknowns take the form

$$[\{x\}]^{2D} = \begin{bmatrix} \{x\}_{1,1} & \{x\}_{1,2} & \{x\}_{1,N} \\ \{x\}_{2,1} & \{x\}_{2,2} & \{x\}_{2,N} \\ & & \\ \{x\}_{M,1} & \{x\}_{M,2} & \{x\}_{M,N} \end{bmatrix}, \tag{4}$$

where $\{x\}_{m,n}$ represents the field coefficients of the array element at row m, column n of the array grid, with $m = 1, 2, \ldots, M$, $n = 1, 2, \ldots, N$. Again, exploiting the Toeplitz property on the planar array, we find that the coupling of the m', n' array element to the m, n element of the array can be uniquely represented as $[a]_{(m-m')(n-n')} = [a]_{p,q}$ since only the distance between elements is of importance. Consequently, the coefficient matrix for planar arrays can be compactly represented as

$$\Pi^{2D} = \begin{bmatrix} [a]_{M-1,1-N} & \cdots & [a]_{M-1,-1} & [a]_{M-1,0} & [a]_{M-1,1} & \cdots & [a]_{M-1,N-1} \\ \vdots & \ddots & & \vdots & & \iddots & \vdots \\ [a]_{1,1-N} & & [a]_{1,-1} & [a]_{1,0} & [a]_{1,1} & & [a]_{1,N-1} \\ [a]_{0,1-N} & \cdots & [a]_{0,-1} & [a]_{0,0} & [a]_{0,1} & \cdots & [a]_{0,N-1} \\ [a]_{-1,1-N} & & [a]_{-1,-1} & [a]_{-1,0} & [a]_{-1,1} & & [a]_{-1,N-1} \\ \vdots & \iddots & & \vdots & & \ddots & \vdots \\ [a]_{1-M,1-N} & \cdots & [a]_{1-M,-1} & [a]_{1-M,0} & [a]_{1-M,1} & \cdots & [a]_{1-M,N-1} \end{bmatrix}. \tag{5}$$

Regardless of array dimensionality (1D, 2D, 3D), the matrix structure will have a Toeplitz property that can be exploited to reduce matrix storage and accelerate matrix-vector product operations. Therefore, the solution of Eq. (1) can be carried out with the block-convolution operation

$$\Pi * \{x\} = \{b\}. \tag{6}$$

For linear arrays, this is a 1D block-convolution, whereas for planar arrays Eq. (6) represents a 2D block-convolution, as described in [10].

4. FINITE COUPLING RADIUS

We now introduce the notation for implementing the finite coupling radius. As mentioned above, we select a desired solution accuracy (such as 2% error) and parametrically determine that such accuracy can be achieved when array element coupling is limited to a radius of influence λ_C, where C represents an effective coupling "cap." This coupling radius will correspond to a maximum coupling term of $[a]_{\pm Cm}$ in the Toeplitz storage scheme. Thus, to mathematically implement the finite coupling radius, we truncate the Toeplitz matrix as

$$\Pi^{1D} = \{[a]_{M-1} \cdots \boxed{[a]_{Cm} \cdots [a]_1 [a]_0 [a]_{-1} \cdots [a]_{-Cm}} \cdots [a]_{1-M}\}, \tag{7}$$

where it is assumed that C_m is smaller than $M - 1$. Removing the truncated terms, this block-vector can be compactly written as

$$\Pi^{1D} = \{[a]_{Cm} \cdots [a]_1 \; [a]_0 \; [a]_{-1} \cdots [a]_{-Cm}\}. \tag{8}$$

Similarly, for the 2D case, the full Toeplitz matrix is reduced from

$$\Pi^{2D} = \begin{bmatrix} [a]_{M-1,1-N} & \cdots & [a]_{M-1,-1} & [a]_{M-1,0} & [a]_{M-1,1} & \cdots & [a]_{M-1,N-1} \\ & \ddots & & \vdots & & \iddots & \\ \vdots & \boxed{\begin{matrix} [a]_{Cm,-Cn} & & [a]_{Cm,0} & & [a]_{Cm,Cn} \\ & \ddots & \vdots & \iddots & \\ [a]_{0,-Cn} & \cdots & [a]_{0,0} & \cdots & [a]_{0,Cn} \\ & \iddots & \vdots & \ddots & \\ [a]_{-Cm,-Cn} & & [a]_{-Cm,0} & & [a]_{-Cm,Cn} \end{matrix}} & \vdots \\ [a]_{1,1-N} & & [a]_{1,-1} & [a]_{1,0} & [a]_{1,1} & & [a]_{1,N-1} \\ [a]_{0,1-N} & \cdots & [a]_{0,-1} & [a]_{0,0} & [a]_{0,1} & \cdots & [a]_{0,N-1} \\ [a]_{-1,1-N} & & [a]_{-1,-1} & [a]_{-1,0} & [a]_{-1,1} & & [a]_{-1,N-1} \\ \vdots & & & \vdots & & & \vdots \\ [a]_{1-M,1-N} & \cdots & [a]_{1-M,-1} & [a]_{1-M,0} & [a]_{1-M,1} & \cdots & [a]_{1-M,N-1} \end{bmatrix}, \tag{9}$$

to

$$\Pi^{2D} = \begin{bmatrix} [a]_{Cm,-Cn} & & [a]_{Cm,0} & & [a]_{Cm,Cn} \\ & \ddots & \vdots & \iddots & \\ & & [a]_{1,-1}\ [a]_{1,0}\ [a]_{1,1} & & \\ [a]_{0,-Cn} & \cdots & [a]_{0,-1}\ [a]_{0,0}\ [a]_{0,1} & \cdots & [a]_{0,Cn} \\ & & [a]_{-1,-1}\ [a]_{-1,0}\ [a]_{-1,1} & & \\ & \iddots & \vdots & \ddots & \\ [a]_{-Cm,-Cn} & & [a]_{-Cm,0} & & [a]_{-Cm,Cn} \end{bmatrix}. \quad (10)$$

Once the terms from outside the coupling radius have been eliminated, the resulting system (for 1D arrays) takes the form

$$\begin{bmatrix} [a]_0 & [a]_1 & \cdots & [a]_{Cm} & 0 & \cdots & 0 \\ [a]_1 & [a]_0 & [a]_1 & \cdots & [a]_{Cm} & 0 & \vdots \\ \vdots & [a]_1 & \ddots & [a]_1 & & \ddots & 0 \\ [a]_{Cm} & \vdots & [a]_1 & [a]_0 & & \vdots & [a]_{Cm} \\ 0 & \ddots & & & \ddots & [a]_1 & \vdots \\ \vdots & 0 & [a]_{Cm} & \cdots & [a]_1 & [a]_0 & [a]_1 \\ 0 & \cdots & 0 & [a]_{Cm} & \cdots & [a]_1 & [a]_0 \end{bmatrix} \times \begin{Bmatrix} \{x\}_1 \\ \{x\}_2 \\ \vdots \\ \{x\}_M \end{Bmatrix} = \begin{Bmatrix} \{b\}_1 \\ \{b\}_2 \\ \vdots \\ \{b\}_M \end{Bmatrix}, \quad (11)$$

which is seen to be a block-banded matrix padded with zeros. It must be stressed that increasing the array size leads to a larger matrix, but the number of "unique" terms remains the same.

As in the standard ADM approach, the matrix-vector product operation in Eq. (11) can be recast and carried out via the convolution operation

$$[A]\{x\} = \{b\} \Rightarrow \Pi * \{x\} = \{b\}. \quad (12)$$

Unfortunately, for the reduced coupling approach, the FFT cannot be efficiently applied without additional storage. That is, the Π vector would have to be zero padded to the original problem size in order to efficiently precompute the FFT [10], and thus no storage savings occurs if the FFT is used.

5. VALIDATION

We have proposed that the mutual coupling within the array environment is largely dominated by elements within a finite radius surrounding any given element of the array. To justify the use of a finite coupling radius, it must be demonstrated that the resulting solution is within a margin of error from the exact solution. Thus, it is necessary to characterize the coupling properties of the desired array element in the environment in which it is to be used. Here, we will validate the coupling properties of a tapered-slot antenna element in a finite-array environment. Due to resource limitations, it is necessary to characterize the antenna element using smaller finite arrays in the 8×8 to 16×16 range. In order to justify the accuracy of this method for very large arrays, it is necessary to show that element coupling properties can be sufficiently characterized with tests in a smaller array environment. To do this, for several such arrays we model the problem using a range of truncated coupling radii and compare the solutions to a reference solution obtained with conventional methods. An indirect solution method is employed in which the solution is correct to within a residual tolerance defined as

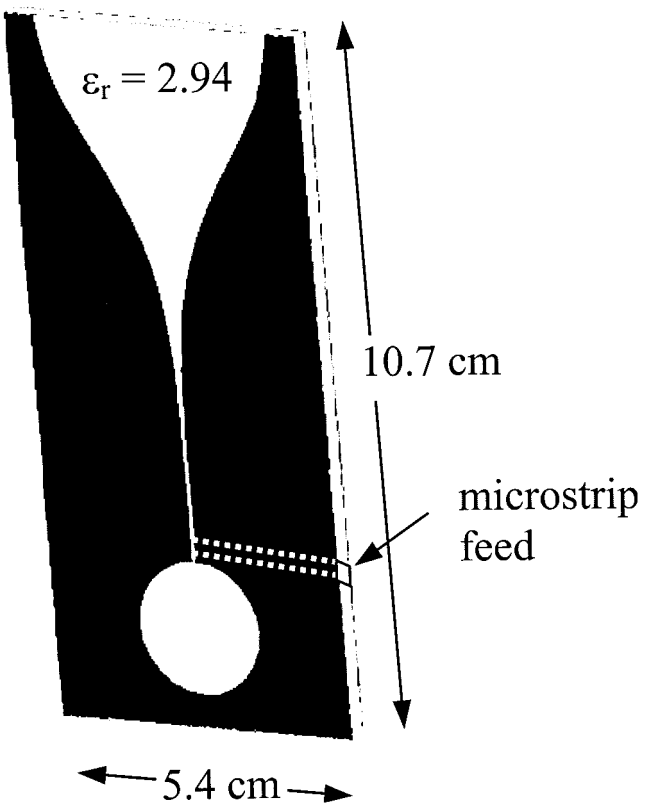

Figure 1 Example of a TSA element

$$\frac{\|\{b\} - [A]\{x\}\|}{\|\{b\}\|} < tol. \quad (13)$$

For the reference solution, *tol* is less than 0.001, and will be denoted as $\{\boldsymbol{E}\}^R$. For the element characterization, the test configurations will consist of various planar arrays of the element, as shown in Figure 1.

This antenna element is a single-sided tapered slot antenna fed via a microstrip line and printed on a 60-mil substrate. The element is modeled with 660 FEM 788 BI unknowns. In the array, the element is rotated 45° to render a triangular or diamond-shaped lattice, as depicted in Figure 2. Also, though the formulation is restricted to arrays with regular grid spacing, the array shape can take any arbitrary form, including circular, elliptical, cross-shaped, and so forth.

For validation, each of the array configurations are modeled with truncated coupling radii that range from encompassing the entire array (accurate solution) to the encompassing only a single element (zero-coupling assumption). The truncated coupling radius (TCR) solution will be denoted as $\{\boldsymbol{E}\}^{TCR}$, and the difference between TCR solutions and the reference solution $\{\boldsymbol{E}\}^R$ can be compute via the relation

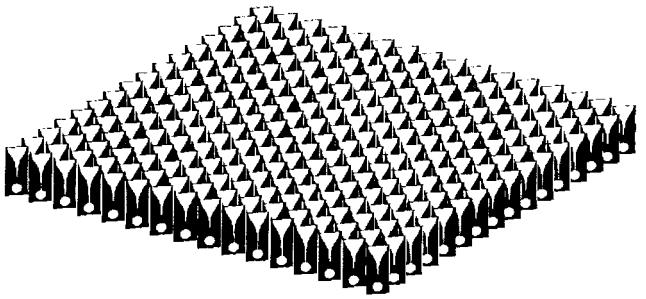

Figure 2 Example of a 16 × 16 TSA array lattice

$$\frac{\|\{\boldsymbol{E}\}^R - \{\boldsymbol{E}\}^{TCR}\|_2}{\|\{\boldsymbol{E}\}^R\|_2} = \frac{\sqrt{\sum ((E_x^R - E_x^{TCR})^2 + (E_y^R - E_y^{TCR})^2 + (E_z^R - E_z^{TCR})^2)}}{\sqrt{\sum ((E_x^R)^2 + (E_y^R)^2 + (E_z^R)^2)}}, \quad (14)$$

where the 3D electric field vector quantities have been sampled at regular intervals throughout the entire problem geometry. Figure 3 shows the comparison of finite-coupling radii solutions to the accurate solution for various array sizes of the same element and same element spacing. As expected, when the coupling radius enlarges, the TCR solution approaches the exact solution. Also, from the curves, it is apparent that a 16 × 16 array is adequate to validate the coupling properties of the antenna element for broadside planar arrays, since the error curves are reasonably close to being bounded by the 16 × 16 data curve. In other words, the effects of array size on the overall error appear to have saturated. We observe that the knee of the error curve is around a radius of 3λ and corresponds to a solution with less than 5% difference from the exact solution. In terms of matrix storage for this problem, the 3λ truncation radius leads to a storage reduction of 99%, or 650 MB as compared to 823 GB for conventional FE-BI or 7.8 GB for a full ADM solution. For larger arrays, the savings will be considerably greater, since the matrix storage for a 3λ truncation radius is still just 650 MB.

Most importantly, this plot indicates that a truncated coupling radius of 3λ will give the same solution accuracy of 5% for virtually any size array.

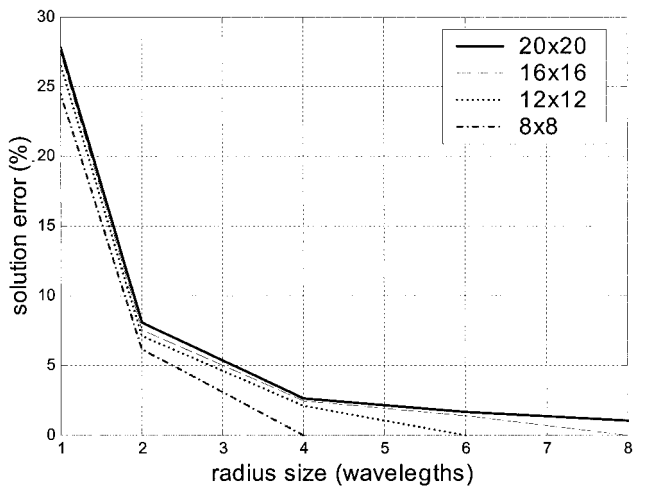

Figure 3 Solution error vs. coupling radius size for various finite arrays

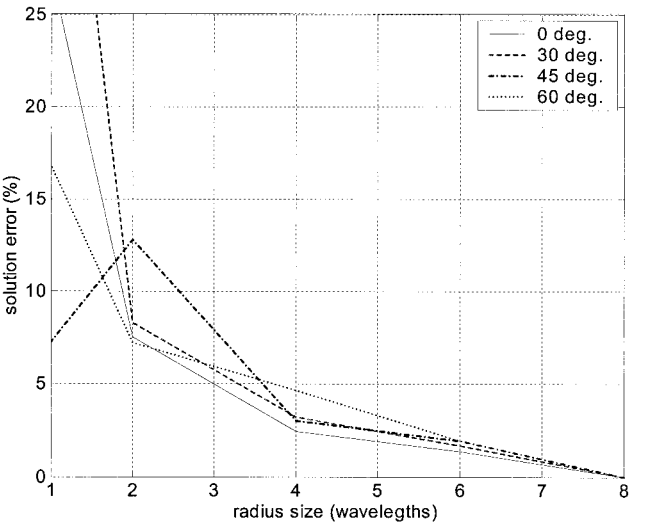

Figure 4 Solution error vs. truncated radius with scanning

In order to justify the validity of this approximation for scanning arrays, Figure 4 shows comparable results for various scan angles using the same element in a 16 × 16 array. As is clearly seen from this plot, when scanning an array, the solution error is slightly affected by scan angle. Thus, for accuracy, it would be safe to use a somewhat larger coupling radius in order to guarantee the same degree of accuracy. Based on the scan results of these plots, we can be reasonably confident that a finite coupling radius of 4λ is sufficient to model very large planar arrays of this antenna element with 5% solution accuracy.

6. LARGE ARRAY SIMULATIONS

The results of Figures 3 and 4 indicate that we can model a much larger finite array using a coupling radius of 3λ–4λ and be reasonably sure that our solution accuracy is within 5% of the exact solution. The reduced coupling radius removes the bottleneck of matrix storage, thus freeing up additional memory for modeling much larger problems. As an example, we consider a 150 × 150 array of the same TSA element as above. We consider here a two-way Taylor weighting distribution with 30-dB sidelobe levels and $\bar{n} = 4$ [13], a result that typically cannot be realized with infinite array analyses. The unknowns required to model this array are 32 million, and the correct solution of such a large system is important in its own right. For the analysis, the coupling radius was truncated to 3λ, which resulted in matrix storage requirements of only 650 MB, or seven orders of magnitude reduction in storage. Storage of the 32 million unknowns alone requires 500 MB. Thus, to store and manipulate the entire problem, consisting of the coupling matrix, the unknown vector, the excitation vector, and solver work vectors, a minimum 9 GB of storage is required (assuming 15 work vectors in the iterative solver). The problem was solved on an HP Itanium server with 16 GB of shared RAM and four 800-MHz processors using an OpenMP-enabled FORTRAN compiler. For a single radiation pattern, such as those shown in Figure 5, the solution time for this 32-million unknowns problem was around 12 h.

The array pattern in Figure 5 is quite typical and is not of any design value. However, the intent of this work is to demonstrate the validity of a technique that can solve extremely large problems beyond conventional solution means. In other words, with this method it is possible to accurately model the edge effects and field distributions of large array structures.

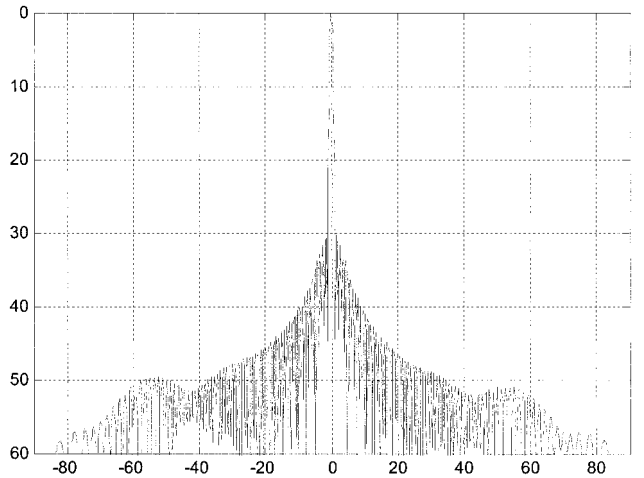

Figure 5 E-plane cuts for the 150 × 150 array, Taylor distribution

7. CONCLUSION

There is no general criterion for choosing a coupling radius that can give a desired accuracy without performing tests. Coupling characteristics are highly dependent upon the type of antenna element, element spacing, or more generally the degree of mutual coupling in the array. The important conclusion from these studies is that once a coupling radius is determined to achieve a given error level, very large finite arrays can be modeled using the proposed TCR method. In combination with Toeplitz storage of the matrix system, the TCR method can be used to "cap" the effective matrix storage so that storage is dependent on the chosen coupling radius and not the overall array size. This is an important concept, because it removes the primary storage bottleneck.

The method presented here has the advantage over infinite approximations of being able to model excitation weighting as well as circular/arbitrarily shaped arrays and correctly accounts for edge effects in finite arrays. Also, this method is valid for array elements of arbitrary shape, whereas infinite-array approximations are typically only valid for geometrically symmetric unit cells. Most importantly, large array problems can be modeled with limited resources on desktop computers.

REFERENCES

1. T.K. Sarkar, E. Arvas, and S.M. Rao, Application of FFT and the conjugate gradient method for the solution of electromagnetic radiation from electrically large and small conducting bodies, IEEE Trans Antennas Propagat 34 (1986), 635–640.
2. T.J. Peters and J.L. Volakis, Application of a conjugate gradient FFT method to scattering from thin planar material plates, IEEE Trans Antennas Propagat 36 (1988), 518–526.
3. J.M. Jin and J.L. Volakis, A biconjugate gradient FFT solution for scattering by planar plates, Electromagn 12 (1992), 105–119.
4. A.P.M. Zwamborn and P.M. van den Berg, A weak form of the conjugate gradient FFT method for plate problems, IEEE Trans Antennas Propagat 39 (1991), 224–228.
5. E. Bleszynski, M. Bleszynski, and T. Jaroszewicz, AIM: Adaptive integral method for solving large scale electromagnetic scattering and radiation problems, Radio Sci 31 (1996), 1225–1251.
6. S. Bindiganavali and J.L. Volakis, Scattering from plates containing small features using the adaptive integral method (AIM), IEEE Trans Antennas Propagat (1998), 1867–1878.
7. W.C. Chew, J.M. Jin, C.C. Lu, E. Michielssen, and J.M. Song, Fast solution methods in electromagnetics, IEEE Trans Antennas Propagat 45 (1997), 533–543.
8. X.Q. Sheng, J.M. Jin, J.M. Song, C.C. Lu, and W.C. Chew, On the formulation of hybrid finite-element and boundary-integral methods for 3D scattering, IEEE Trans Antennas Propagat 46 (1998), 303–311.
9. R. Kindt, K. Sertel, E. Topsakal, and J.L. Volakis, A domain decomposition of the finite element-boundary integral method for finite array analysis, Applied Computational Electromagnetics Society Annual Review, Monterey, CA, 2002, pp 103–109.
10. R. Kindt, K. Sertel, E. Topsakal, and J.L. Volakis, Array decomposition method for the accurate analysis of finite arrays, to appear in IEEE Trans Antennas Propagat, May 2003.
11. J.L. Volakis, A. Chatterjee, and L.C. Kempel, Finite element method for electromagnetics. New York: IEEE Press, 1998.
12. Y. Saad, Iterative methods for sparse linear systems. New York, NY: PWS Publishing, 1996.
13. A.T. Villeneuve, Taylor patterns for discrete arrays, Trans IEEE AP-32 (1984), 1089–1093.

RADOME-PROTECTED LOW-PROFILE GSM ANTENNA ON SMALL GROUND PLANE

Lakhdar Zaid and Robert Staraj
Laboratoire d'Electronique, Antennes et Télécommunications
Université de Nice-Sophia Antipolis, CNRS UPRESA 6071
Bât. 4, 250 rue A. Einstein, 06560 Valbonne, France

Received 3 February 2003

ABSTRACT: *A small radiating element, designed to work in the GSM frequency band, made up entirely of square parts on air substrate is described. The dimensions of the ground plane are only 1.3 times the dimensions of the radiating element. By stacking two square wire patches, the characteristics of compactness, large bandwidth, and monopolar wire radiation pattern can be achieved. Circular designs have been already been presented, however, compared to the circular plates solution, the new structure described in this paper allows an easier realization as well as a protective dielectric radome. Owing to its low-profile, low-cost, and radioelectric properties such as large bandwidth and dipolar-type radiation pattern, this antenna is very suitable for automobile or indoor ceiling applications which require a very small ground plane.* © 2003 Wiley Periodicals, Inc. Microwave Opt Technol Lett 38: 328–331, 2003; Published online in Wiley InterScience (www.interscience.wiley.com). DOI 10.1002/mop.11051

Key words: *microstrip antennas; wire-patch antennas; miniature antennas; GSM antennas*

1. INTRODUCTION

The intensive development and large number of wireless applications have increased the need for special antenna designs. In the study of mobile antennas, we can distinguish two domains. The first and more frequently described concerns the study of antennas dedicated to mobile phone handsets. Effectively, recent patch antenna research has focused on reducing the size of the radiating element concurrently with the respect to the standard frequency bandwidth, generally in spite of radiation pattern and gain. The second domain concerns automobile or indoor ceiling applications where the most common antenna requirements are generally and simultaneously, low-cost, light-weight, and low-profile designs with large-bandwidth and high-performance monopolar-type radiation. Fortunately, it has been shown that microstrip antennas can be used below their classical fundamental modes by including ground wires connecting the radiating patches to the ground plane [1, 2]. Concurrently, stacked elements are also a well-known